# EFFECT OF EVAPORATION-CONDENSATION ON PHOTOACOUSTICS OF AEROSOLS

## FINAL REPORT

## GRANT NUMBER: N00014-99-1-0912

SUBMITTED TO:

OFFICE OF NAVAL RESEARCH
800 NORTH QUINCY STREET
ARLINGTON, VA 22217-5660

by

Richard Raspet and William V. Slaton
National Center for Physical Acoustics
University of Mississippi
University, MS 38677

and

W. Patrick Arnott
Desert Research Institute
Atmospheric Sciences Center
2215 Raggio Parkway
Reno, NV 89215-1095

NCPA Report LF0700-01

JULY 5, 2000

20000720 011

DTIC QUALITY INSPECTED 4

# REPORT DOCUMENTATION PAGE

| 1. AGENCY USE ONLY *(Leave Blank)* | 2. REPORT DATE 07 Jul 00 | 3. REPORT DYPE AND DATES COVERED Final 01 Jul 99 to 30 Jun 00 |
|---|---|---|

**4. TITLE AND SUBTITLE**
Effect of Evaporation-Condensation on Photoacoustics of Aerosols

**5. FUNDING NUMBERS**
PE 61153N
G N00014-99-1-0912

**6. AUTHOR(S)**
Richard Raspet, Wiliam V. Slaton and W. Patrick Arnott

**7. PERFORMING ORGANIZATION NAME(S) AND ADDRESS(ES)**
Jamie L. Whitten National Center for Physical Acoustics
The University of Mississippi
University, MS 38677

**8. PERFORMING ORGANIZATION REPORT NUMBER**

**9. SPONSORING / MONITORING AGENCY NAME(S) AND ADDRESS(ES)**
Office of Naval Research
ONR 331
800 North Quincy Street
Arlington, VA 22217-5660

**10. SPONSORING / MONITORING AGENCY REPORT NUMBER**

**11. SUPPLEMENTARY NOTES**

**12a. DISTRIBUTION / AVAILABILITY STATEMENT**
Approved for public release; Distribution unlimited

**12b. DISTRIBUTION CODE**

**13. ABSTRACT** *(Maximum 200 words)*
This document reports on the preliminary investigation of relative humidity effects on light absorption by aerosols. The Desert Research Institute took part in the Southern Great Plains Radiation Measurement and took simultaneous measurements of photoacoustic light absorption and light absorption measured by filter methods as a function of relative humidity. The variation in relative humidity was controlled artificially. This work is described in detail in Section I. A detailed theory of the effect or evaporation-condensation on photoacoustic output has been developed at the University of Mississippi. This theory is valid over a wide span of particle sizes, particle densities and operating frequencies. This work is presented in Section II.

**14. SUBJECT TERMS** Photoacoustics, relative humidity, light absorption, aerosols, evaporation, condensation

**15. NUMBER OF PAGES** 32s

**16. PRICE CODE**

| 17. SECURITY CLASSIFICATION OF REPORT UNCLASSIFIED | 18. SECURITY CLASSIFICATION OF THIS PAGE UNCLASSIFIED | 19. SECURITY CLASSIFICATION OF ABSTRACT UNCLASSIFIED | 20. LIMITATION OF ABSTRACT |
|---|---|---|---|

NSN 7540-01-280-5500

Standard Form 298 (Rev. 2-89)
Prescribed by ANSI Std. Z39-1
298-102

## TABLE OF CONTENTS

# EFFECT OF EVAPORATION-CONDENSATION
## ON PHOTOACOUSTICS OF AEROSOLS

## FINAL REPORT

## SUMMARY

This preliminary investigation of relative humidity effects on light absorption by aerosols has been very successful. The Desert Research Institute (DRI) took part in the Southern Great Plains Radiation Measurement and took simultaneous measurements of photoacoustic light absorption and light absorption measured by filter methods as a function of relative humidity. The variation in relative humidity was controlled artificially. This work is described in detail in Section I.

A detailed theory of the effect of evaporation-condensation on photoacoustic output has been developed at the University of Mississippi. This theory is valid over a wide span of particle sizes, particle densities and operating frequencies. This work is presented in Section II.

Richard Raspet, Pat Arnott and Hans Moosmüller met at DRI in May 2000 to coordinate the research effects and to plan future cooperative research. The measurements and theory will be combined in the near future in the preparation of papers for publication, of experimental design and of proposals for future research.

## 1. RELATIVE HUMIDITY DEPENDENCE OF LIGHT ABSORPTION

The photoacoustic instrument is used to obtain light absorption by aerosols, with applications relevant to radiation transfer in the atmosphere, or more specifically, electro-optical imaging and sensing. The photoacoustic instrument has the potential for obtaining the relative humidity dependence of light absorption, whereas more common filter methods cannot provide a quantitative measure due to moisture deposition on the substrate. For dry aerosols (RH<50%), the sound generated in the instrument is due to the conversion to heat of the light absorbed by the aerosols. The aerosols are sufficiently small that this heat transfers entirely to the surrounding air during the acoustic period.

1

However, for moist aerosols, vapor may be released from the heated aerosols, in addition to heat. In the general case, the sound pressure level is due to both heat and mass transfer.

The contribution of mass transfer to the sound pressure level measured in a photoacoustic instrument was investigated by performing measurements and theoretical analysis. The photoacoustic instrument was transported to the Department of Energy, Southern Great Plains Atmospheric Radiation Measurement in north central Oklahoma (abbreviated as SGP). An "aerosol trailer," among others, is located at the SGP, and the purpose of this trailer is to measure optical and physical properties of atmospheric aerosol. In particular, personnel from NOAA in Boulder, CO operate a system to vary the relative humidity (RH) of the incoming air from 40% to 95%. This RH conditioner has been evaluated by NOAA, and provided a very convenient means to accomplish the experimental component of the effort. Ancillary instruments also present in the trailer were useful in quantifying aerosol properties before the humidity conditioner. The relative humidity dependence of light absorption has not been directly measured in the past due to the use of filter-based methods. The photoacoustic instrument was described previously,[1,2] and the calibration can be verified with nitrogen dioxide gas.[3]

The data set from this project is outstanding. DRI personnel were present for the project (the entire month of March, 2000), and the aerosol trailer was operated during this time to ensure good data quality. A synopsis follows.

1. Aerosol light absorption measurements with 3 instruments.
    a. Normal psap filter based instrument used at SGP.
    b. Extra psap sitting on the humidified inlet.
    c. DRI photoacoustic instrument on the humidified inlet.

2. Light absorption for dry and humidified aerosols was measured. Light absorption measurements are among the more difficult to do. A great combination of aerosols was available:
    a. Cases of very clean air (background)
    b. Cases of long-range transport of probably vehicle exhaust (tractors, interstate, roads, etc, mostly diesel perhaps?)

2

c. Cases of smoke plumes from farmer's fires.

3. Findings to date are:

a. The photoacoustic data correlates well with the DRY psap measurements. However, the exact value for light absorption is not settled yet. (Slope of correlation is not one, but appears to be around 1.6, with the photoacoustic instrument reporting less light absorption than the other instrument).

b. The photoacoustic data show no increase of light absorption with increase of RH, and perhaps a decrease. (Theory suggests perhaps a factor of 2 increase for carbon cores coated with an aqueous layer. But are light absorbing aerosols hygroscopic?)

c. The humidified PSAP shows erroneously high light absorption as the RH increases due to the filter taking on aqueous solution from scattering aeroso. When the RH goes back down, this psap shoots erroneously negative as well. It is very good that the SGP crew uses a dry psap for their measurements on a routine basis. It also calls into question all measurements ever taken with a psap at elevated RH, including those done on aircraft.

To evaluate the light absorption dependence, the ratio of light absorption obtained by the photoacoustic instrument to that of the dry psap was computed and averaged over the entire data set. This ratio is deemed the f(RH) function for light absorption, and is a dimensionless value. If f(RH) increases as the RH increases, than the conclusion is that light absorption increases with RH as the aerosols swell and moisten with increased RH. It may also be that the chain aggregate structure of the carbonaceous aerosol collapses upon humidification. Another potential effect is that RH increases cause aerosol losses in the sample lines to increase. It should be kept in mind that the analogous f(RH) for scattering by aerosols is in the range of 2 to 4 for the RH around 95%.

Figure 1 shows the measured f(RH) for a 1 μm inlet on the sample line. First, the average ratio is around 0.6, indicating that the psap light absorption is larger than the photoacoustic value. It would be unity if both instruments reported the same light absorption. This calibration issue is likely to be traced to the psap calibration method. Next, note that the f(RH) function decreases with RH. This decrease could be due to at least the following three factors:

1. The sample lines begin to absorb particles as the RH increases.

2. Mass transfer is less efficient at producing sound than is heat transfer, so the photoacoustic instrument could report less light absorption for elevated RH. Theory should provide a bound for this efficiency difference.

3. Aerosol morphological changes could lower the mass absorption efficiency if the chain aggregate particles of soot collapse upon humidification.

Figure 2 shows the measured f(RH) for a 10 μm inlet used on the sample line, allowing larger particles through the system. Note that the f(RH) function drops off faster with increasing RH for this inlet (i.e. larger aerosol) than it does for the 1 μm inlet.
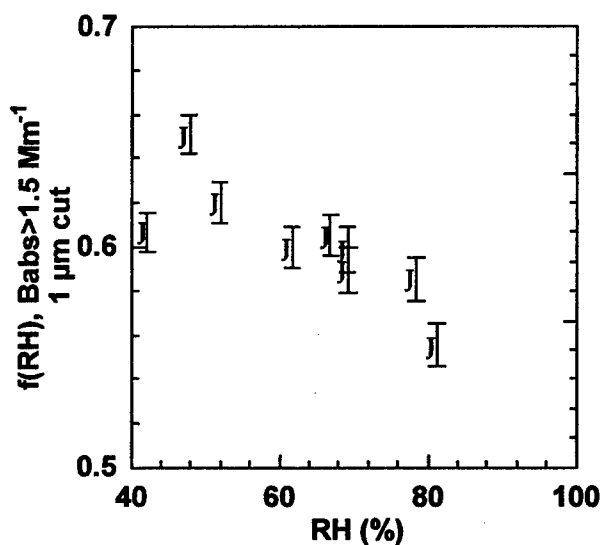


Figure 1. Ratio of photoacoustic and dry psap light absorption as a function of relative humidity. The inlet line had a 1 μm cut to prevent larger particles from entering. The line is a least-squares fit to the data, and is included to illustrate the trend (not to hypothesize a linear relationship.)
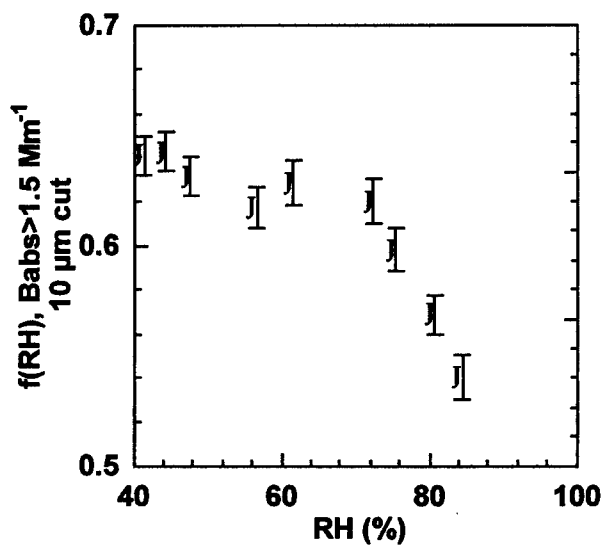
Figure 2. Same as Fig. 1, though the inlet size cut allowed particles smaller than 10 μm to pass through the instruments. Note the relatively smaller ratio in this figure at high RH, when compared with that of Fig. 1.

In summary, the relative humidity dependence of light absorption was measured as a function of relative humidity using a photoacoustic instrument, and for dry aerosol using a filter-based instrument. The data suggests that RH increases are associated with a decrease in light absorption. Three hypotheses have been provided for the mechanism of decrease. The data set will be further analyzed, and compared with theory.

## 2. THEORY OF THE EFFECT OF EVPORATION-CONDENSATION ON PHOTOACOUSTIC OUTPUT

### 2.1 Introduction

DRI has developed photoacoustic spectrometers for the measurement of light absorption by atmospheric aerosols.[1,2] A laser source is chopped near the resonant frequency of an acoustic resonator containing the sample. The light absorbed by the aerosol in the beam heats the surrounding gas, driving the acoustic wave in the resonator. The sound pressure level in the resonator is a measure of the light absorption. The results of this technique have been compared to those from an aethalometer, a device that measures the absorption of particles gathered on a filter medium. DRI is interested in the effects of relative humidity on the adsorption of light by aerosols and on the effect of volatile components on the calibration of the photoacoustic instrument.

M.B. Baker analyzed the effect of evaporation–condensation on the photoacoustics of volatile aerosols in a non-resonant cell.[4] Baker's analysis assumes that the aerosol particles do not interact and that the photoacoustic cell is non-resonant. In this paper, we allow for high aerosol particle number density effects and perform the Green's function source analysis as appropriate for resonant cells. The analysis is based on the low reduced frequency method used previously to evaluate the effects of evaporation–condensation on sound propagation in wet walled tubes.[5,6]

### 2.2 Theory

The DRI photoacoustic cell is a flow through cell. The laser beam is much smaller than the area of the resonate tube. We therefore assume that the residence time of the droplets in the beam is small compared with the time for significant DC mass evaporation to occur. The laser excitation can be considered as a DC component producing steady evaporation and heating and an AC component that will alternately heat and cool the droplet. Our analysis will concentrate on the AC component. In addition, we assume that each droplet of radius $r_0$ is surrounded by similar neighbors and that drop

5

inertia is high enough that each droplet supplies heat and vapor into its neighborhood of radius $a = 1/n^{1/3}$ where n is the aerosol particle density in m$^{-3}$.

The governing equations are the Navier-Stokes equation, the continuity equation for each component and for the mixture, the equation of state for the mixture, the entropy equation for the mixture, and the diffusion equation for the mixture. In linearized form these are:[7,8]

$$\rho_o \frac{\partial \vec{v}}{\partial t} = -\nabla p + \mu \nabla^2 \vec{v} + \left( \beta + \frac{1}{3} \mu \right) \nabla (\nabla \cdot \vec{v}),$$

(1)

$$\frac{\partial \rho_1}{\partial t} + \rho_1^o (\nabla \cdot \vec{v}_1) = 0,$$

(2a)

$$\frac{\partial \rho_2}{\partial t} + \rho_2^o (\nabla \cdot \vec{v}_2) = 0,$$

(2b)

$$\frac{\partial \rho}{\partial t} + \rho_o (\nabla \cdot \vec{v}) = 0,$$

(2c)

$$-\frac{\partial p}{\partial t} + \frac{\gamma}{\gamma - 1} nk \frac{\partial T}{\partial t} - \kappa \nabla^2 T + k_T nkT \nabla \cdot (\vec{v}_1 - \vec{v}_2) = 0,$$

(3)

$$\frac{\partial p}{\partial t} = nk \frac{\partial T}{\partial t} + kT_o \left( \frac{1}{m_1} \frac{\partial \rho_1}{\partial t} + \frac{1}{m_2} \frac{\partial \rho_2}{\partial t} \right),$$

(4)

and

$$\vec{v}_1 - \vec{v}_2 = D_{12} \left( \frac{1}{\rho_2^o} \nabla \rho_2 - \frac{1}{\rho_1^o} \nabla \rho_1 - \frac{n}{\rho_o P_o} (m_2 - m_1) \nabla p - \frac{n^2}{n_1 n_2} \cdot \frac{k_T}{T_o} \nabla T \right).$$

(5)

In these equations, variables, $\rho_1, \rho_2$, are the density of the gas and of the vapor; $\rho = \rho_1 + \rho_2$ is the density of the mixture; $\vec{v}_1, \vec{v}_2$ are the hydrodynamic velocity of the gas and of the vapor; $\vec{v} = (\rho_1 \vec{v}_1 + \rho_2 \vec{v}_2)/\rho$ is the hydrodynamic velocity of the mixture; p is the pressure of the mixture; and T is the temperature of the mixture. In the above equations, constant $\mu$ is the viscosity of the mixture;

$\beta$ is the bulk viscosity of the mixture; $m_1, m_2$ are the molecular mass of gas and vapor; $n_1, n_2$ are the number density of the gas and of the vapor; $n = n_1 + n_2$ is the total number density; $\gamma_1, \gamma_2$ are the ratio of specific heats of the gas and of the vapor; $n\gamma/(\gamma-1) = n_1\gamma_1/(\gamma_1-1) + n_2\gamma_2/(\gamma_2-1)$ is the ratio of $nc_p/R$ for the mixture; $c_p$ is the molar heat capacity at constant pressure; $R$ is the universal gas constant; $\kappa$ is the thermal conductivity of the mixture; $D_{12}$ is the mass diffusion coefficient; $k_T$ is the thermal diffusion ratio, as defined in Ref. 8, page 541; and $k$ is the Boltzmann's constant.

The linearized heat equation for the droplet is given by,

$$\frac{\partial}{\partial t}\left(\rho_L c_{pL} T_L\right) - \kappa_L \nabla^2 T_L = Q(t), \tag{6}$$

where $\rho_L$ is the liquid density; $c_{pL}$ is the liquid heat capacity at constant pressure; $\kappa_L$ is the heat conductivity; $T_L$ is the temperature of the liquid; and $Q(t)$ is the energy absorbed from the laser per unit time per unit volume in the drop. Assuming single frequency excitation, we set $Q(t) = Q_o e^{-i\omega t}$, where $Q_o = \alpha I_o$ with the absorption coefficient for the drop given by $\alpha$ and the intensity of the laser light given by $I_o$. We assume that the absorption of light energy is small enough so that the drop is evenly heated. We assume also that the resulting diffusion and heat flow will be predominately radial and define two dimensionless variables,

$$\eta = \frac{r}{a}, \tag{7}$$

the dimensionless radius, and the reduced frequency,

$$\Omega = \frac{\omega a}{c}. \tag{8}$$

7

Assuming that all the variables have an $e^{-i\omega t}$ time dependence, where $\omega$ is the angular frequency of the modulated laser beam, we introduce normalized variables as follows:

$$p = \frac{\rho_o c^2}{\gamma}\left(1.0 + p^* e^{-i\omega t}\right),$$
(9a)

$$T = T_o\left(1.0 + T^* e^{-i\omega t}\right),$$
(9b)

$$T_L = T_o\left(1 + T_L^* e^{-i\omega t}\right),$$
(9c)

$$\vec{v} = c\,\vec{v}^*\, e^{-i\omega t},$$
(9d)

and

$$\vec{v}_1 - \vec{v}_2 = c\,\vec{V}^*\, e^{-i\omega t},$$
(9e)

where c is the sound speed in the mixture.

Using the definitions above, the Navier-Stokes equation becomes

$$\frac{1}{\gamma}\frac{\partial p^*}{\partial \eta} - i\Omega v^* - \frac{1}{\eta^2}\frac{\partial}{\partial \eta}\left(\frac{1}{\eta^2}\frac{\partial\left(\eta^2 v^*\right)}{\partial \eta}\right) = 0,$$
(10)

where $\lambda_\mu = a\sqrt{\omega\rho\Big/\left(\beta + \frac{4}{3}\mu\right)}$. Note that this definition of the dimensionless viscous wave number is not

the same as the shear wave number defined in Ref 5. The entropy equation is given by,

$$\Omega\frac{\gamma-1}{\gamma}p^* - \Omega T^* + i\frac{\Omega}{\lambda_T^2}\frac{1}{\eta^2}\frac{\partial}{\partial \eta}\left(\eta^2\frac{\partial T^*}{\partial \eta}\right) - \frac{\gamma-1}{\gamma}\frac{k_T}{\eta^2}\frac{\partial\left(\eta^2 V^*\right)}{\partial \eta} = 0,$$
(11)

where $\lambda_T = a\sqrt{\dfrac{\rho\omega c_p}{\kappa}}$. The equation of state is combined with the continuity equations of each

component to form the equation of state in terms of $p^*$, $T^*$, $v^*$ and $V^*$:

$$\Omega p^* - \Omega T^* + \frac{i}{\eta^2} \frac{\partial(\eta^2 v^*)}{\partial \eta} - i \frac{n_1 n_2}{n \rho_o}(m_1 - m_2)\frac{1}{\eta^2}\frac{\partial(\eta^2 V^*)}{\partial \eta} = 0. \tag{12}$$

The final equation results from combining the diffusion equation with the continuity relations;

$$V^* - \frac{i}{\lambda_D^2}\frac{\partial}{\partial \eta}\left(\frac{1}{\eta^2}\frac{\partial(\eta^2 v^*)}{\partial \eta}\right) - \frac{\Omega}{\lambda_D^2}\left[\frac{n}{\rho_o}(m_1 - m_2)\frac{\partial p^*}{\partial \eta} - \frac{n^2 k_T}{n_1 n_2}\frac{\partial T^*}{\partial \eta}\right] = 0, \tag{13}$$

where $\lambda_D = a\sqrt{\omega/D_{12}}$ . The temperature equation in the droplet is,

$$T_L^* - \frac{i}{\lambda_L^2}\frac{1}{\eta^2}\frac{\partial}{\partial \eta}\left(\eta^2 \frac{\partial T_L^*}{\partial \eta}\right) = \frac{iQ_o}{c_{pL}\rho_L \omega T_o}, \tag{14}$$

where $\lambda_L = a\sqrt{\frac{\rho_L \omega c_{pL}}{\kappa_L}}$ . Note this is defined with respect to the neighborhood radius a, not with respect to the drop radius $r_0$. We can eliminate $p^*$ from the gas-vapor mixture equations resulting in the following equations. Eqs. (11) and (12) form,

$$\frac{\Omega}{\gamma - 1}\left[T^* - i\frac{\gamma}{\lambda_T^2}\frac{1}{\eta^2}\frac{\partial}{\partial \eta}\left(\eta^2 \frac{\partial T^*}{\partial \eta}\right)\right] + \frac{i}{\eta^2}\frac{\partial(\eta^2 v^*)}{\partial \eta} - i\left[\frac{n_1 n_2}{n \rho_o}(m_1 - m_2) - k_T\right]\frac{1}{\eta^2}\frac{\partial(\eta^2 V^*)}{\partial \eta} = 0. \tag{15}$$

Eqs. (10) and (13) are combined to form,

$$\frac{\Omega}{\lambda_D^2}\frac{n^2 k_T}{n_1 n_2}\frac{\partial T^*}{\partial \eta} - i\gamma\frac{\Omega^2}{\lambda_D^2}\frac{n}{\rho_o}(m_1 - m_2)\left[v^* - \frac{i}{\lambda_\mu^2}\frac{\partial}{\partial \eta}\left(\frac{1}{\eta^2}\frac{\partial(\eta^2 v^*)}{\partial \eta}\right)\right] + \left[V^* - \frac{i}{\lambda_D^2}\frac{\partial}{\partial \eta}\left(\frac{1}{\eta^2}\frac{\partial(\eta^2 V^*)}{\partial \eta}\right)\right] = 0. \tag{16}$$

Finally, we eliminate $\frac{\partial p^*}{\partial \eta}$ from Eq. (10) and take the $\eta$ derivative of Eq. (12) to obtain

$$-\Omega\frac{\partial T^*}{\partial \eta}+\left[i\Omega^2 v^*+\left(i+\frac{\Omega^2\gamma}{\lambda_\mu^2}\right)\frac{\partial}{\partial\eta}\left(\frac{1}{\eta^2}\frac{\partial(\eta^2 v^*)}{\partial\eta}\right)\right]-i\frac{n_1 n_2}{n\rho_o}(m_1-m_2)\frac{\partial}{\partial\eta}\left(\frac{1}{\eta^2}\frac{\partial(\eta^2 V^*)}{\partial\eta}\right)=0. \tag{17}$$

At this point, we note that the reduced frequency, $\Omega$, is small, even for low number density and high operating frequency. ($\Omega \cong 0.04$ for $n = 350$ particles/cm$^3$ and $f = 2000$ Hz). Accordingly, we drop all terms in $\Omega^2$ from the equations:

$$\frac{\Omega}{\gamma-1}\left[T^*-i\frac{\gamma}{\lambda_T^2}\frac{1}{\eta^2}\frac{\partial}{\partial\eta}\left(\eta^2\frac{\partial T^*}{\partial\eta}\right)\right]+\frac{i}{\eta^2}\frac{\partial(\eta^2 v^*)}{\partial\eta}-i\left[\frac{n_1 n_2}{n\rho_o}(m_1-m_2)-k_T\right]\frac{1}{\eta^2}\frac{\partial(\eta^2 V^*)}{\partial\eta}=0, \tag{18}$$

$$\frac{\Omega}{\lambda_D^2}\frac{n^2 k_T}{n_1 n_2}\frac{\partial T^*}{\partial\eta}+\left[V^*-\frac{i}{\lambda_D^2}\frac{\partial}{\partial\eta}\left(\frac{1}{\eta^2}\frac{\partial(\eta^2 V^*)}{\partial\eta}\right)\right]=0, \tag{19}$$

and

$$-\Omega\frac{\partial T^*}{\partial\eta}+i\frac{\partial}{\partial\eta}\left(\frac{1}{\eta^2}\frac{\partial(\eta^2 v^*)}{\partial\eta}\right)-i\frac{n_1 n_2}{n\rho_o}(m_1-m_2)\frac{\partial}{\partial\eta}\left(\frac{1}{\eta^2}\frac{\partial(\eta^2 V^*)}{\partial\eta}\right)=0. \tag{20}$$

The term containing $v^*$ can be eliminated by combining Eqs. (18) and (20):

$$\frac{\partial T^*}{\partial\eta}-\frac{i}{\lambda_T^2}\frac{\partial}{\partial\eta}\left(\frac{1}{\eta^2}\frac{\partial}{\partial\eta}\left(\eta^2\frac{\partial T^*}{\partial\eta}\right)\right)+i\frac{\gamma-1}{\gamma}\frac{k_T}{\Omega}\frac{\partial}{\partial\eta}\left(\frac{1}{\eta^2}\frac{\partial(\eta^2 V^*)}{\partial\eta}\right)=0. \tag{21}$$

Equations (19) and (21) are coupled, second order differential equations for $\dfrac{\partial T^*}{\partial\eta}$ and $V^*$. The coupling is provided by the thermal diffusion ratio, $k_T$, that appears in the entropy equation from diffusion across the control volume and in the diffusion equation for temperature driven diffusion.

These equations, combined with boundary conditions and the temperature equation in the drop, represent a complete solution. The effect of the coupling on air-water mixtures has been investigated

in Ref 6. For photoacoustics in the atmosphere, the mole fraction of vapor will be very low (less than 0.05) and the effect of the coupling of the diffusion and thermal wave numbers low. In Ref 6, the calculated fractional change in thermal and diffusive wave numbers for water vapor in air is less than $10^{-4}$ for temperatures up to 30°C. The use of the low reduced frequency approximation and the modal analysis of Ref 6 demonstrates that Baker's use of simplified hydrodynamic equations is justified for this analysis for higher frequency devices. The boundary conditions for the solution of this problem are developed within these approximations. Diffusion and thermal effects are assumed to dominate the acoustic terms in the droplet neighborhood.

## 2.3 Boundary Conditions

The boundary conditions at the neighborhood boundary (r = a) are

$$V^*(1) = 0,$$  (22a)

and,

$$\left. \frac{\partial T^*}{\partial \eta} \right|_{\eta=1} = 0.$$  (22b)

At the drop radius, $r_o$, the temperature must be continuous; the heat generated by condensation at the surface must be carried away by the heat flux into the gas and droplet; and the diffusion velocity can be calculated from the temperature at the drop radius. We require that the temperature in the drop, $T_L^*$, and the gas mixture, $T^*$, be equal at the drop radius ($\eta = r_o/a$):

$$T^* = T_L^*.$$  (23)

Next, we require heat flux balance at the drop radius. In general, this can be written as,

$$\vec{q} = \kappa \vec{\nabla} T - \kappa_L \vec{\nabla} T_L, \tag{24}$$

where $\vec{q}$ is the heat flux generated at the boundary. For a system undergoing a phase change at the wall, the heat flux generated is written, $\vec{q} = \ell \vec{m}_{flux} = \ell \rho_2^0 \vec{v}_2(\frac{r_o}{a})$, where $\rho_2^0$ is the ambient vapor density; $\vec{v}_2(\frac{r_o}{a})$ is the radial velocity of the vapor evaluated at the wall; and $\ell$ is the latent heat of vaporization. Thus, our boundary condition for the heat flux at $\eta = r_o/a$ becomes,

$$\ell \rho_2^0 \vec{v}_2 = \kappa \vec{\nabla} T - \kappa_L \vec{\nabla} T_L. \tag{25}$$

Use of the definition of the radial difference velocity, $V^*$, yields the following equation for the heat flux,

$$-\ell \rho_2^0 \frac{c V^* R}{T_o}\bigg|_{\eta = r_o/a} = \left[ \kappa \frac{\partial T^*}{\partial \eta} - \kappa_L \frac{\partial T_L^*}{\partial \eta} \right]_{\eta = r_o/a}. \tag{26}$$

Temperature fluctuations at the drop radius induce vapor pressure fluctuations. The Clausius-Clapeyron equation,[9]

$$p_{Vapor}\big|_{\eta = r_o/a} = p_o \exp\left[ -\frac{\ell m_2}{\mathbf{R}} \left( \frac{1}{T} - \frac{1}{T_{REF}} \right) \right]_{\eta = r_o/a}, \tag{27}$$

relates the vapor pressure to the temperature. An expression for the density of species 2 near the tube wall can be derived from the ideal gas law and Eq. (27):

$$\rho_2\big|_{\eta = r_o/a} = \rho_2^0 \frac{T_{REF}}{T} \exp\left[ -\frac{\ell m_2}{\mathbf{R}} \left( \frac{1}{T} - \frac{1}{T_{REF}} \right) \right]_{\eta = r_o/a}. \tag{28}$$

Linearizing with $T = T_o\left(1 + T^* e^{-i\omega t}\right)$ yields,

$$\rho_2\big|_{\eta={r_o}/a} = \rho_2^0\left(1+\left(\frac{\ell\,m_2}{\mathbf{R}\,T_0}-1\right)T^*e^{-i\omega t}\right)_{\eta={r_o}/a},\qquad(29)$$

where $T_o$ is the ambient temperature of the system. The equation of continuity can be used to write Eq. (29) in terms of $V^*$ and $T^*$:

$$i\frac{1}{\eta^2}\frac{\partial}{\partial\eta}\left(\eta^2 V^*\right)\bigg|_{\eta={r_o}/a} = \Omega\left(\frac{\ell\,m_2}{\mathbf{R}\,T_0}-1\right)T^*\bigg|_{\eta={r_o}/a}.\qquad(30)$$

The divergence of $v^*$ is dropped from this boundary condition since $v^*$ at the boundary is smaller than $V^*$ by the ratio $\rho_2/\rho$ and $v^*$ is principally an acoustic wave with small spatial variation compared to diffusion and heat conduction.[10] The fourth boundary condition is that the time rate of heat flow out of the drop at $r_0$ must equal the time rate of change in internal energy in the drop neighborhood,

$$4\pi\,r_o^2\,\frac{\kappa}{a}\frac{\partial T^*}{\partial\eta}\bigg|_{{r_o}/a} = -i\omega\int_{r_o/a}^1 c_v\rho T^*(\eta)4\pi a^3\eta^2 d\eta.\qquad(31)$$

Again, this boundary condition is only correct if the acoustic energy emission is negligible with respect to the internal energy.

## 2.4 Solution

The set of differential equations to be solved are,

$$\frac{\partial T^*}{\partial\eta} - \frac{i}{\lambda_T^2}\frac{\partial}{\partial\eta}\left(\frac{1}{\eta^2}\frac{\partial}{\partial\eta}\left(\eta^2\frac{\partial T^*}{\partial\eta}\right)\right) = 0,\qquad(32)$$

13

$$V^* - \frac{i}{\lambda_D^2} \frac{\partial}{\partial \eta} \left( \frac{1}{\eta^2} \frac{\partial \left( \eta^2 V^* \right)}{\partial \eta} \right) = 0, \tag{33}$$

and

$$T_L^* - \frac{i}{\lambda_L^2} \frac{1}{\eta^2} \frac{\partial}{\partial \eta} \left( \eta^2 \frac{\partial T_L^*}{\partial \eta} \right) = \frac{i Q_o}{c_{pL} \rho_L \omega T_o}. \tag{34}$$

The solutions are in terms of spherical Bessel and Hankel functions. We choose solutions so that $T_L^*$ is finite at $r = 0$ and so that $\dfrac{\partial T^*}{\partial \eta}$ and $V^*$ are zero at $r = a$. The solutions are,

$$\frac{\partial T^*}{\partial \eta} = A f_1 \left( \sqrt{i} \lambda_T \eta \right), \tag{35}$$

$$V^* = B f_1 \left( \sqrt{i} \lambda_D \eta \right), \tag{36}$$

and

$$T_L^* = D j_0 \left( \sqrt{i} \lambda_L \eta \right) + i \frac{Q_o}{c_{pL} \rho_L \omega T_o}. \tag{37}$$

A, B and D are constants to be determined from the boundary conditions. $f_1 \left( \sqrt{i} \lambda \eta \right)$ and $f_0 \left( \sqrt{i} \lambda \eta \right)$ are defined as,

$$f_1 \left( \sqrt{i} \lambda \eta \right) = -\lambda^2 \eta_o^2 \left( h_1^{(1)} \left( \sqrt{i} \lambda \eta \right) - h_1^{(2)} \left( \sqrt{i} \lambda \eta \right) \frac{h_1^{(1)} \left( \sqrt{i} \lambda \right)}{h_1^{(2)} \left( \sqrt{i} \lambda \right)} \right), \tag{38}$$

and

$$f_0 \left( \sqrt{i} \lambda \eta \right) = i \sqrt{i} \lambda \eta_o \left( h_0^{(1)} \left( \sqrt{i} \lambda \eta \right) - h_0^{(2)} \left( \sqrt{i} \lambda \eta \right) \frac{h_1^{(1)} \left( \sqrt{i} \lambda \right)}{h_1^{(2)} \left( \sqrt{i} \lambda \right)} \right), \tag{39}$$

14

where $\eta_o = r_o/a$. The functions $f_1$ and $f_0$ are chosen so that they approach one for the small drop, large neighborhood limit. This facilitates comparison with Baker's theory. Recursion relations for the spherical Bessel functions give,

$$\frac{1}{\eta^2}\frac{\partial}{\partial\eta}\left(\eta^2 f_1\left(\sqrt{i}\lambda\eta\right)\right) = i\lambda^2\eta_o f_o\left(\sqrt{i}\lambda\eta\right), \tag{40}$$

$$\frac{\partial}{\partial\eta}\left(f_0\left(\sqrt{i}\lambda\eta\right)\right) = -\frac{f_1(\eta)}{\eta_o}, \tag{41}$$

and

$$\frac{\partial}{\partial\eta}\left(\frac{1}{\eta^2}\frac{\partial}{\partial\eta}\left(\eta^2 f_1\left(\sqrt{i}\lambda\eta\right)\right)\right) = -i\lambda^2 f_1\left(\sqrt{i}\lambda\eta\right). \tag{42}$$

Integration of Eq. (35) gives,

$$T^*(\eta) = -\eta_o A f_0\left(\sqrt{i}\lambda_T\eta\right) + C, \tag{43}$$

where C is an additional undetermined constant. This term arises due to the finite neighborhood assumption. Using this form in Eq. (31) gives,

$$A\frac{4\pi r_o^2\kappa}{a}f_1\left(\sqrt{i}\lambda_T\eta_o\right) = i\omega\int_{\eta_o}^1 c_v\rho\left[-\eta_o A f_0\left(\sqrt{i}\lambda_T\eta\right) + C\right]4\pi a^3\eta^2 d\eta. \tag{44}$$

Performing the integration yields,

$$A\frac{4\pi r_o^2\kappa}{a}f_1\left(\sqrt{i}\lambda_T\eta_o\right) = -i\omega c_v\rho\left[-\frac{iAr_o^3}{\lambda_T^2}f_1\left(\sqrt{i}\lambda_T\eta_o\right) + \frac{a^3 C}{3}\left(1 - \eta_o^3\right)\right]. \tag{45}$$

Solving for C we find,

$$C = \frac{3iA\kappa}{\omega c_v \rho a^4} f_1\left(\sqrt{i}\lambda_T \eta_o\right) \frac{1 - \frac{\eta_o}{\gamma}}{1 - \eta_o^3}. \tag{46}$$

Usually $\eta_o^3$ is negligible. C tends to zero as a goes to infinity. The equation for the temperature $T^*$ is given by,

$$T^*(\eta) = -\eta_o A\left[f_0\left(\sqrt{i}\lambda_T \eta\right) - \delta f_1\left(\sqrt{i}\lambda_T \eta_o\right)\right], \tag{47}$$

where $\delta = \frac{3i\kappa}{\omega c_v \rho} \frac{r_o}{a^3} \frac{1 - \frac{\eta_o}{\gamma}}{1 - \eta_o^3}$. This term is small for all aerosols of interest. $\frac{3\kappa}{c_v \rho} \approx 4 \times 10^{-5}$ for saturated air/water at 30°C. The spatially constant temperature fluctuations in the neighborhood of the drop are negligible. In the following, we set $\delta = 0$. The temperature matching boundary condition, Eq. (23), becomes

$$D j_0\left(\sqrt{i}\lambda_L \eta_o\right) + \frac{iQ_o}{c_{pL}\rho_L \omega T_o} = -\eta_o A f_0\left(\sqrt{i}\lambda_T \eta_o\right). \tag{48}$$

The heat flux boundary condition, Eq. (26), becomes

$$-\frac{\ell \rho_2^0 c}{T_o} B f_1\left(\sqrt{i}\lambda_D \eta_o\right) = \frac{\kappa}{a} A f_1\left(\sqrt{i}\lambda_T \eta_o\right) + \frac{\kappa_L}{a} \sqrt{i}\lambda_L D j_1\left(\sqrt{i}\lambda_L \eta_o\right). \tag{49}$$

The boundary condition that expresses the vapor pressure in terms of the surface temperature of the drop gives,

$$\lambda_D^2 \eta_o B f_0\left(\sqrt{i}\lambda_D \eta_o\right) = \Omega\left(\frac{\ell m_2}{RT_0} - 1\right) \eta_o A f_0\left(\sqrt{i}\lambda_T \eta_o\right). \tag{50}$$

16

Eliminating D from Eqs. (48) and (49), we find that

$$\frac{\kappa}{a}Af_1\left(\sqrt{i}\lambda_T\eta_o\right)+\frac{\ell\rho_2^0c}{T_o}Bf_1\left(\sqrt{i}\lambda_D\eta_o\right)=\sqrt{i}\lambda_L\frac{\kappa_L}{a}\frac{j_1\left(\sqrt{i}\lambda_L\eta_o\right)}{j_0\left(\sqrt{i}\lambda_L\eta_o\right)}\left[\frac{iQ_o}{c_{pL}\rho_L\omega T_o}+\eta_oAf_0\left(\sqrt{i}\lambda_T\eta_o\right)\right].\tag{51}$$

The product $\lambda_L\eta_o$ is usually small; small argument expansions can be used to express Eq. (51) in simpler form.

Let $c'=\dfrac{3}{\sqrt{i}\lambda_L\eta_o}\dfrac{j_1\left(\sqrt{i}\lambda_L\eta_o\right)}{j_0\left(\sqrt{i}\lambda_L\eta_o\right)}\cong1+\dfrac{i}{15}(\lambda_L\eta_o)^2$.  The second expression results from the small

argument expansion and demonstrates that $c'$ can be taken as 1 unless $\lambda_L\eta_o$ is of O(1).  For 100 μm

drop of water at 2000 Hz this value is 2.3, at 20 Hz, Baker's assumed value it is 0.07.  Gathering terms,

we find,

$$\frac{\kappa}{a}Af_1\left(\sqrt{i}\lambda_T\eta_o\right)\left[1-i\frac{c_{pL}\rho_L\omega r_o^2c'}{3\kappa}\frac{f_0\left(\sqrt{i}\lambda_T\eta_o\right)}{f_1\left(\sqrt{i}\lambda_T\eta_o\right)}\right]+\frac{\ell\rho_2^0c}{T_o}Bf_1\left(\sqrt{i}\lambda_D\eta_o\right)=-\frac{Q_oc'a}{3T_o}.\tag{52}$$

From Eq. (50),

$$B=\left[\frac{D_{12}}{ac}\left(\frac{\ell m_2}{\mathbf{R}T_0}-1\right)\frac{f_0\left(\sqrt{i}\lambda_T\eta_o\right)}{f_0\left(\sqrt{i}\lambda_D\eta_o\right)}\right]A.\tag{53}$$

Eq. (52) is solved for A:

$$A=-\frac{Q_oc'r_oa}{3\kappa T_of_1\left(\sqrt{i}\lambda_T\eta_o\right)}\frac{1}{\Xi},\tag{54}$$

where,

$$\Xi=1-i\frac{c_{pL}\rho_L\omega r_o^2c'}{3\kappa}\frac{f_0\left(\sqrt{i}\lambda_T\eta_o\right)}{f_1\left(\sqrt{i}\lambda_T\eta_o\right)}+\frac{\ell\rho_2^0D_{12}}{\kappa T_o}\left(\frac{\ell m_2}{\mathbf{R}T_0}-1\right)\frac{f_0\left(\sqrt{i}\lambda_T\eta_o\right)}{f_1\left(\sqrt{i}\lambda_T\eta_o\right)}\frac{f_1\left(\sqrt{i}\lambda_D\eta_o\right)}{f_0\left(\sqrt{i}\lambda_D\eta_o\right)}.\tag{55}$$

These constants may be combined with Eqs. (35) and (36) to evaluate $\dfrac{\partial T^*}{\partial \eta}$ and $V^*$. For the present investigation of photoacoustics, we evaluate the acoustic source terms rather than the variables $\dfrac{\partial T^*}{\partial \eta}$ and $V^*$.

The wave equation with mass injection and heat injection is given by[11]

$$\nabla^2 P - \frac{1}{c^2}\frac{\partial^2 P}{\partial t^2} = -f(\vec{r},t),\tag{56}$$

where

$$f(\vec{r},t) = \frac{\partial}{\partial t}\left(M + \frac{\gamma-1}{c^2}H\right) = -i\omega\left(M + \frac{\gamma-1}{c^2}H\right).\tag{57}$$

$M$ is the mass injected per unit time and volume; $H$ is the heat energy added per unit time and volume.

The mass injected per unit time per unit volume is calculated by the product of $\rho_2 v_2$ at the drop surface times the surface area divided by the neighborhood volume with $v_2 = -cV^*$. This gives

$$M = \left(\frac{r_o}{a}\right)^3 \frac{Q_o c' \rho_2^0 D_{12}}{\kappa T_o \Xi}\left(\frac{\ell m_2}{\mathbf{R} T_0} - 1\right)\frac{f_0\left(\sqrt{i}\lambda_T\eta_o\right)}{f_1\left(\sqrt{i}\lambda_T\eta_o\right)}\frac{f_1\left(\sqrt{i}\lambda_D\eta_o\right)}{f_0\left(\sqrt{i}\lambda_D\eta_o\right)}.\tag{58}$$

The heat energy injected per unit time per unit volume is determined by summing the heat flux over the surface divided by the neighborhood volume:

$$H = \left(\frac{r_o}{a}\right)^3\frac{Q_o c'}{\Xi}.\tag{59}$$

For weakly absorbing drops, $Q_o$ is the product of the beam intensity and the liquid absorption in inverse meters. The optical absorption length due to the aerosol is given by the absorption in the

18

droplet times the volume ratio $(r_o/a)^3$. The phase of $f(\vec{r},t)$ will be the phase of the resulting pressure wave with respect to the phase of the laser intensity.

## 2.5 Analysis

Equations (58) and (59) along with Eq. (55) have been written to facilitate comparison with Baker's low frequency, small particle, large spacing results.[4] Her results are recovered by setting

$$c' = 1 , \tag{60a}$$

$$\frac{f_0\left(\sqrt{i}\lambda_T\eta_o\right)}{f_1\left(\sqrt{i}\lambda_T\eta_o\right)}\frac{f_1\left(\sqrt{i}\lambda_D\eta_o\right)}{f_0\left(\sqrt{i}\lambda_D\eta_o\right)} = 1 , \tag{60b}$$

and

$$-i\frac{c_{pL}\rho_L\omega r_o^2 c'}{3\kappa}\frac{f_0\left(\sqrt{i}\lambda_T\eta_o\right)}{f_1\left(\sqrt{i}\lambda_T\eta_o\right)} = 0 . \tag{60c}$$

Eq. (60a) expresses the condition that the droplet radius is smaller than a thermal penetration depth in the droplet; that is, the temperature is spatially uniform in the drop. Eq. (60b) expresses two conditions. The first is that the finite drop neighborhood does not affect the heat and mass transfer at the drop surface. This condition will be met if the neighborhood radius is more than a thermal penetration depth in the gas. The second condition inherent in Eq. (60b) is that $\lambda_L\eta_o$ be small enough so that the leading terms in the small argument expansion for $h_0$ and $h_1$ are sufficient. This is due to the normalization of $f_0$ and $f_1$ retaining only the leading terms (see Eqs. (38) and (39)).

Figure 3 displays the magnitude and phase of the ratio in Eq. (60b) versus the neighborhood radius for two particle sizes, 1 μm and 10 μm for typical frequencies for Baker's study and for DRI instrumentation. The ratio is significantly different from one only when the neighborhood radius is the

19

size of a thermal penetration depth. At 2000 Hz, this only occurs for particle densities of 240 cm$^{-3}$ corresponding to a particle spacing of 10$^{-3}$ m.
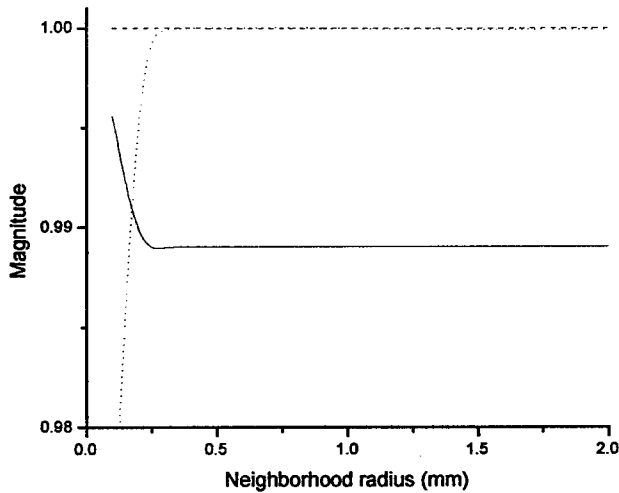


Figure 3a. Magnitude of the ratio in Eq. (60b) as a function of neighborhood radius for different operating frequencies and drop sizes. 2000 Hz and 10 micron sized drop (solid line); 200 Hz and 0.1 micron sized drop (dashed line); 20 Hz and 1 micron sized drop (dotted line). The ambient air pressure is 1 atm and the ambient temperature is 290 K.
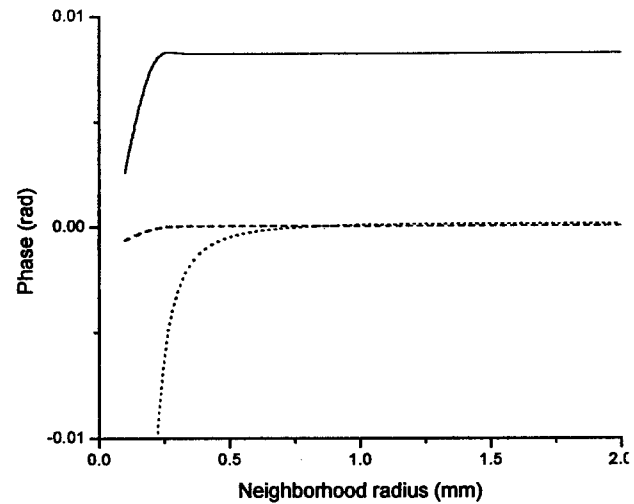
Figure 3b. Phase of the ratio in Eq. (60b) as a function of neighborhood radius for different operating frequencies and drop sizes. 2000 Hz and 10 micron sized drop (solid line); 200 Hz and 0.1 micron sized drop (dashed line); 20 Hz and 1 micron sized drop (dotted line). The ambient air pressure is 1 atm and the ambient temperature is 290 K.

The last condition, Eq. (60c), is violated in higher frequency instruments. The magnitude and phase of $f_0\left(\sqrt{i}\lambda_T\eta_o\right)/f_1\left(\sqrt{i}\lambda_T\eta_o\right)$ for the same cases as Fig. 3 is displayed in Fig. 4. These ratios are near constant and real for particle densities less than 240 cm$^{-3}$. The 10 μm drop at low frequencies is affected by the next term in the expansion of $h_0$ and $h_1$. The magnitude of this term is O(1) none-the-less. The full term in Eq. (60c) can have a significant effect on the acoustic level for the high frequency device and is frequency dependent. This term is due to the change in magnitude and phase of the surface temperature due to heat conduction into the gas. As the frequency increases, more heat energy is conducted from the particle and the temperature variation at the surface decreases and changes phase with respect to the laser excitation. Chan[12] has discussed this effect in regard to thermal blooming from high intensity laser beams in aerosols. When this term is neglected, the ratio of the heat and mass term in the source equation is frequency independent. The inclusion of Eq. (60c) in the formulation provides a diagnostic for experimental investigation of mass transfer on photoacoustics.

20
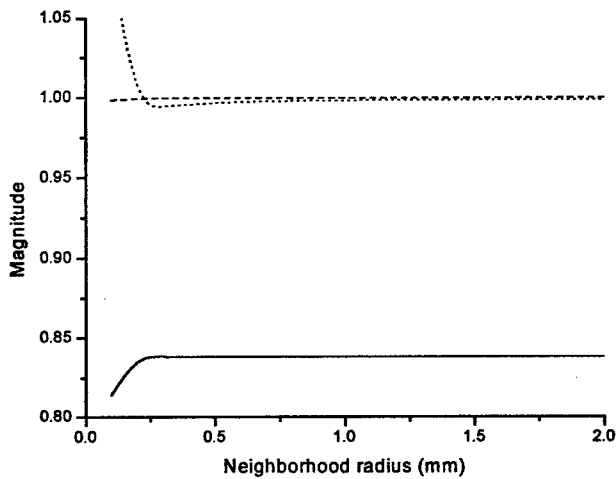
Figure 4a. Magnitude of the ratio $f_0\left(\sqrt{i}\lambda_T\eta_o\right)/f_1\left(\sqrt{i}\lambda_T\eta_o\right)$ as a function of neighborhood radius for different operating frequencies and drop sizes. 2000 Hz and 10 micron sized drop (solid line); 200 Hz and 0.1 micron sized drop (dashed line); 20 Hz and 1 micron sized drop (dotted line). The ambient air pressure is 1 atm and the ambient temperature is 290 K.
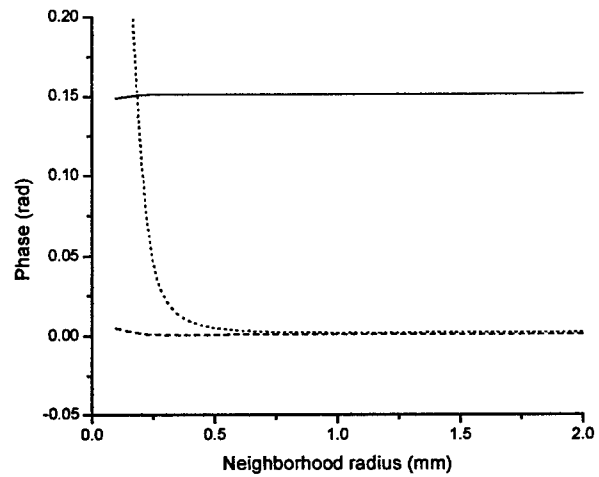
Figure 4b. Phase of the ratio $f_0\left(\sqrt{i}\lambda_T\eta_o\right)/f_1\left(\sqrt{i}\lambda_T\eta_o\right)$ as a function of neighborhood radius for different operating frequencies and drop sizes. 2000 Hz and 10 micron sized drop (solid line); 200 Hz and 0.1 micron sized drop (dashed line); 20 Hz and 1 micron sized drop (dotted line). The ambient air pressure is 1 atm and the ambient temperature is 290 K.

Figure 5 shows the magnitude and phase of the acoustic source strength for 1 μm water drops in saturated air at 290 K. In this figure, we set $Q_o = 1$. Also shown is the magnitude and phase of the photoacoustic source strength per unit volume for an identical particle with no latent heat (a non-volatile particle) and the magnitude of the individual contribution to the volatile source.
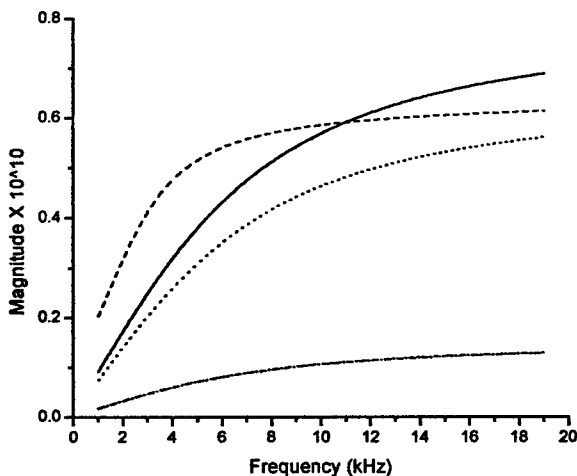


Figure 5a. Magnitude of the acoustic source strength for a single drop as a function frequency for 1 micron sized drops. Total effect (solid line); Heat contribution (dotted line); Mass contribution (dash-dot line); Total effect without latent heat (dashed line). The ambient air pressure is 1 atm and the ambient temperature is 290 K.
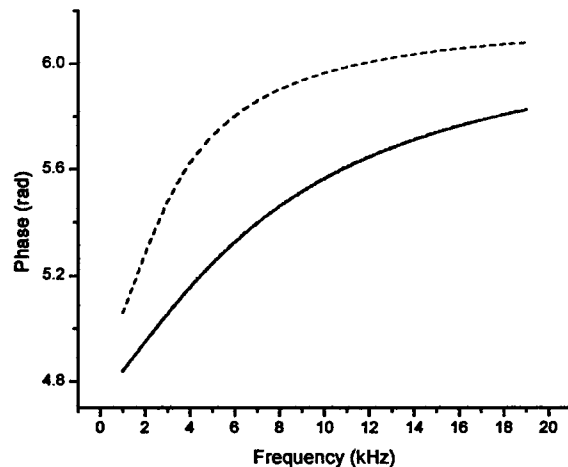
Figure 5b. Phase of the acoustic source strength for a single drop as a function frequency for 1 micron sized drops. Total effect (solid line); Heat contribution (dotted line); Mass contribution (dash-dot line); Total effect without latent heat (dashed line). The ambient air pressure is 1 atm and the ambient temperature is 290 K.

21

At lower frequencies, the second term in $\Xi$ is negligible and the volatile particle source strength is smaller than the non-volatile source strength. The cooling of the particle by evaporation reduces the temperature variation at the drop surface and therefore reduces both the amount of heat conducted into the gas and the amount of mass injected. At high frequencies, the cooling of the drop surface due to conduction into the gas becomes dominant over cooling due to evaporation. The magnitude of the thermal source alone approaches that of the thermal source of the non-volatile particle. The mass injected into the gas then adds into the heat flux term to increase the photoacoustic signal.

A transition from the source strength being linearly dependent on frequency to near constant as $\omega$ is increased is observed. The position of the transition depends on the size of the terms in Eq. (55). The second term is the only term that is sensitive to the frequency and to the particle size, other than the leading $(r_o/a)^3$ term in Eqs. (57) and (58) that just expresses the volumetric fraction occupied by light absorbing material. The phase of the photoacoustic signal varies from $3\pi/2$ to $2\pi$ as the second term in Eq. (55) increases in size.

## 2.6 Applications

These equations can be applied to estimate the effect of thin layers of adsorbed volatile liquids on the photoacoustics of solid particles. It is expected, for example, that water will be adsorbed onto carbon particles at vapor pressures below saturation. If we assume fractional coverage, f, of the solid by the liquid and the heat capacity and mass of the liquid is small with respect to those of the drop, the photoacoustics source strength can be determined by Eqs. (57), (58) and (59) with the following substitution: $c_{pL} \rightarrow c_{pS}$, the specific heat of the solid, and $\rho_L \rightarrow \rho_S$, the density of the solid. In addition, the factor f is introduced into Eq. (49). This introduces the factor f as reducing $M$ and in reducing the third factor in Eq. (55). This also assumes that the solid particles are spherical.

## 2.7 Conclusions

A theory of photoacoustics for volatile aerosols for arbitrary acoustic frequencies has been developed. Correction terms for larger particles and for high particle densities have been included in the analysis. At high frequencies, a term not included in Baker's analysis is significant.

The contribution of evaporation to the photoacoustic measurements of light adsorption can be determined using Eqs. (55), (57), (58) and (59). If the changes necessary to describe fractional liquid coverage on a solid substrate particle are incorporated, the source strength contains four unknowns, assuming that the identity and properties of the liquid-vapor species is known. Two measurements of magnitude and phase of the source strength at widely spaced frequencies are sufficient to determine whether evaporation-condensation is occurring on the absorbing particles and to evaluate the size of that contribution. Multifrequency measurements would, of course, provide more information.

## 3. REFERENCES

[1] W. Patrick Arnott, Hans Moosmüller, C. Fred Rogers, Tianfeng Jin, Reinhard Bruch, "Photoacoustic Spectrometer for Measuring Light Absorption by Aerosol: Instrument Description," Atmos. Environ. **33**, (1999) 2845-2852.

[2] H. Moosmüller, W.P. Arnott, C.F. Rogers, J.C. Chow, C.A. Frazier, L.E. Sherman, D.L. Dietrich, "Photoacoustic and Filter Measurements Related to Aerosol Light Absorption During the Front Range Air Quality Study (Colorado 1996/1997)," J. Geo. Res. **103**, D21, 28149-28157 (1998).

[3] W. P. Arnott, H. Moosmüller, and J. W. Walker, "Nitrogen dioxide and kerosene-flame soot calibration of photoacoustic instruments for measurement of light absorption by aerosols," Rev. Sci. Ins. June_Submittal. (2000).

[4] W.B. Baker, "Energy Absorption by Volatile Atmospheric Aerosol Particles," Atmos. Environ. **10**, (1976) 241-248.

[5]Richard Raspet, Craig J. Hickey, James M. Sabatier, "The Effect of Evaporation-Condensation on Sound Propagation in Cylindrical Tubes Using the Low Reduced Frequency Approximation," J. Acoust. Soc. Am. **105**, (1999) 65-73.

[6]Craig J. Hickey, Richard Raspet, William V. Slaton, "Effects of Thermal Diffusion on Sound Attenuation in Evaporating and Condensing Gas Vapor Mixtures in Tubes," J. Acoust. Soc. Am. **107**, (2000) 1126-1130.

[7]L.D. Landau and E.M. Lifshitz, *Fluid Mechanics*, (Butterworth–Heinemann, Oxford 1997), 2nd Ed.

[8]J.V. Hirschfelder, C. Curtiss, R. B. Bird, *Molecular Theory of Gases and Liquids*, (Wiley, New York, 1954).

[9]F. Reif, *Fundamentals of Statistical and Thermal Physics*, (McGraw – Hill, New York, 1965).

[10]Alan D. Pierce, *Acoustics, An Introduction to its Physical Principles and Applications*, (Acoustical Society of America, Woodbury, NY 1989). Characteristics of the vorticity, acoustical and entropy modes are described on pages 519-531.

[11]Philip M. Morse and K. Uno Ingard, *Theoretical Acoustics*, (Princeton University Press, Princeton NJ 1986). Radiation of sound from a small region with violent fluid motion is analyzed on pages 322-325.

[12]C.H. Chan, "Effective Absorption for Thermal Blooming Due to Aerosols," Appl. Phys. Letters **26**, 1975, 628-629.